

RELATIVISTIC ELECTRON PRECIPITATION VARIATIONS ON MANNED SPACECRAFT

Tsvetan Dachev¹, Borislav Tomov¹, Yury Matviichuk¹, Plamen Dimitrov¹, Nikolay Bankov¹,
Jordanka Semkova¹, Rositsa Koleva¹,
Vladislav Petrov², Viacheslav Shurshakov², Victor Benghin²

¹Space Research and Technology Institute – Bulgarian Academy of Sciences
e-mail: tdachev@bas.bg, btomov@bas.bg, ymat@bas.bg, pdimitrov1957@abv.bg, ngb43@abv.bg,
jsemkova@stil.bas.bg, rkoleva@stil.bas.bg

²State Research Center Institute of Biomedical problems – Russian Academy of Sciences
e-mail: petrov@imbp.ru, shurshakov@inbox.ru, v_benghin@mail.ru

Keywords: Space radiation, Space weather, Dosimetry, Spectrometry

Abstract: The paper presents observations of radiation environment variations, including relativistic electron precipitations (REP) on the “Mir” and the International Space Station (ISS). Data were obtained by 5 Bulgarian-built instruments flown in 1989-1994, 2001 and 2008-2010. The first data are from the Liulin instrument flown 1989-1994 inside the Russian “Mir” space station. This period, being in high solar activity, is dominated by a large number of solar proton events (SPE) and magnetic storms, which generate a large number of inner magnetosphere enhancements, including the formation of the “New” radiation belt at low L values after the sudden commencement of a magnetic storm (SSC) at 03:42 UT on 24 March 1991. The “New” belt was observed by us till the middle of 1993. The second period of observations is in May-August 2001 inside the USA laboratory module of the ISS. Last, the February 2008 - August 2010 period was analyzed. The REP in April 2010, being the second largest in GOES history (with a >2 MeV electron fluence event), is specially studied. The L value profiles of the radiation environment inside and outside the “Mir” and the ISS space stations was plotted and analyzed. These long-term observations support the conclusion that REP is a common phenomenon on manned spacecraft. REP and the dose rates variations generated by them inside and outside the manned spacecraft have to be specially studied because of the space radiation risk, which they induce to the crew members during extravehicular activities.

ВАРИАЦИИ НА ИЗСИПВАЩИТЕ СЕ РЕЛАТИВИСТКИ ЕЛЕКТРОНИ РЕГИСТРИРАНИ НА ПИЛОТИРАНИ КОСМИЧЕСКИ КОРАБИ

Цветан Дачев¹, Борислав Томов¹, Юрий Матвийчук¹, Пламен Димитров¹, Николай Банков¹,
Йорданка Семкова¹, Росица Колева¹,
Владислав Петров², Вячеслав Шуршаков², Виктор Бенгин²

¹Институт за космически изследвания и технологии – Българска академия на науките
e-mail: tdachev@bas.bg, btomov@bas.bg, ymat@bas.bg, pdimitrov1957@abv.bg, ngb43@abv.bg,
jsemkova@stil.bas.bg, rkoleva@stil.bas.bg

²Държавен изследователски център, Институт за медуко-биологически науки – Руска академия на науките
e-mail: petrov@imbp.ru, shurshakov@inbox.ru, v_benghin@mail.ru

Ключови думи: Космическа радиация, Космическо време, Дозиметрия, Спектрометрия

Резюме: В статията са анализирани вариациите на радиационната среда, включително тези по време на изсипване на релативистки електрони (ИРЕ) на станцията „МИР“ и на Международната космическа станция (МКС). Данните от 5 прибора, разработени в България, са получени в периодите 1991, 2001 and 2008-2010 г. Първите данни са от прибора ЛЮЛИН, летял на станцията „Мир“ в периода 1988-1994 г. Този период е във висока слънчева активност и доминиран от голям брой Слънчеви протонни събития (СПС) и магнитни бури, които генерират голям брой увеличения във вътрешната магнитосфера, включително формиране на „Нов“ радиационен пояс на ниски ширини след внезапното начало на магнитна буря в 03:42 UT на 24 Март 1991 г. „Новият“ пояс беше наблюдаван от нас до средата на 1993 г. Вторият период на наблюдения е вътре във лабораторния модул на САЩ на

МКС през м. май 2001 г. Последните наблюдения са в периода февруари 2008-август 2010 г. ИРЕ през м. април 2010, които са вторите по големина в наблюденията на електронни потоци с енергия повече от 2 MeV, са специално изучени. Профилите на радиационното обкръжение на станциите „Мир“ и МКС в зависимост от стойността на L са анализирани. Тези дългопериодични наблюдения поддържат заключението, че ИРЕ са обичайно явление на орбиталните станции. Те, заедно с вариациите на мощността на дозата, трябва да бъдат специално изучавани заради радиационния риск, които те представляват за членовете на екипажите по време на дейности извън стените на станциите.

1. Introduction

The radiation field around and inside the ISS is complex, composed by galactic cosmic rays (GCR), trapped radiation of the Earth radiation belts, solar energetic particles, albedo particles from Earth's atmosphere and secondary radiation produced in the shielding materials of the spacecraft or the space suit and in the biological objects. The radiation field at a location, either outside or inside the spacecraft is affected both by the shielding and the surrounding materials (Badhwar et al., 1998; Benton and Benton, 2001; NCRP, Report No. 142, 2002). Dose characteristics in low-Earth orbits (LEO) depend also on many other parameters such as the spacecraft orbit parameters, the solar cycle phase, the current helio and geophysical parameters.

1.1 Galactic cosmic rays

The dominant radiation component in the ISS radiation environment is the GCR modulated by the altitude and the geomagnetic coordinates of the station. The GCR are not rays at all but charged particles that originate from sources beyond the Solar System. They are thought to be accelerated at the highly energetic sources like neutron stars, black holes and supernovae within our Galaxy. GCR are the most penetrating among the major types of ionizing radiation (Mewaldt, 1996). The flux and spectra of GCR particles show modulation, which is anti-correlated with the solar activity. The distribution of GCR is believed to be isotropic throughout the interstellar space. The energies of GCR particles range from several tens up to 10^{12} MeV nucleon⁻¹. The GCR spectrum consists of 98% protons and heavier ions (baryon component) and 2% electrons and positrons (lepton component). The baryon component is composed of 87% protons, 12% helium ions (alpha particles) and 1% heavy ions (Simpson, 1983). Highly energetic particles in the heavy ion component, typically referred to as high Z and energy (HZE) particles, play a particularly important role in space dosimetry (Benton and Benton, 2001) and affected strongly the biological objects and humans in space (Horneck, 1994). HZE particles, especially iron, possess high LET and are highly penetrating, giving them a large potential for radiobiological damage (Kim et al., 2010). The daily average GCR absorbed dose rates measured with R3DE (Dachev et al. 2012a) outside of the ISS vary in the range 77-102 $\mu\text{Gy day}^{-1}$ with an average of 91 $\mu\text{Gy day}^{-1}$.

1.2 Trapped radiation belts

Radiation belts are the regions of high concentration of the energetic electrons and protons trapped within the Earth's magnetosphere. There are two distinct belts of toroidal shape surrounding the Earth where the high energy charged particles get trapped in the Earth's magnetic field. Energetic ions and electrons within the Earth's radiation belts pose a hazard to both astronauts and spacecraft's electronic. The inner radiation belt, located between about 0.1 to 2 Earth radii, consists of both electrons with energies up to 10 MeV and protons with energies up to ~ 200 MeV. The South-Atlantic Anomaly (SAA) is an area where the inner radiation belt comes closer to the Earth surface owing to a displacement of the magnetic dipole axes from the Earth's center. The daily average SAA absorbed dose rates measured with R3DE instrument (Dachev et al. 2012a) outside of the ISS vary in the range 110-685 $\mu\text{Gy day}^{-1}$ with an average of 426 $\mu\text{Gy day}^{-1}$. The maximal hourly SAA absorbed dose rates reached 1500-1600 $\mu\text{Gy h}^{-1}$. It was found (Dachev et al., 2011) that the docking of the US Space Shuttle with ISS decreases strongly the SAA doses because of the additional shielding, which the 78-tons body of the Shuttle provides against the inner radiation belt protons.

The outer radiation belt (ORB) starts from about 4 Earth radii and extends up to about 9-10 Earth radii in the anti-sun direction. The outer belt mostly consists of electrons whose energy is not larger than 10 MeV. Relativistic electrons enhancements in the outer radiation belt are one of the major manifestations of space weather (Zheng et al., 2006; Wrenn, 2009) at near Earth's orbit. These enhancements occur mainly after magnetic storms. The electron flux may cause problems for components located outside a spacecraft (e.g. solar cell degradation). They do not have enough energy to penetrate a heavily shielded spacecraft such as through the ISS wall, but may deliver large additional doses to astronauts during Extravehicular Activity (EVA) (Dachev et al., 2009a, 2012b and 2012c). The average ORB dose rate measured with the R3DE (Dachev et al. 2012a) outside of the ISS is 8.64 $\mu\text{Gy day}^{-1}$, and the range is between 0.25 and 212 $\mu\text{Gy day}^{-1}$. Rare sporadic fluxes of

relativistic electrons were measured with the R3DR instrument to deliver as high absorbed doses as $20000 \mu\text{Gy h}^{-1}$.

2. Instruments description

Five different Liulin type instruments were used in this study. The first one was the LIULIN instrument (Dachev et al., 1989) flown inside “Mir” space station in the 1988-1994 time span behind more than 20 g cm^{-2} shielding. The instrument was developed for the scientific program of the second Bulgarian cosmonaut – Alexander Alexandrov. *The period mentioned above, being in high solar activity, was dominated by large number of solar proton events (SPE) and magnetic storms. These conditions generated a large number of inner magnetosphere enhancements, including the formation of the “New radiation belt” (Shurshakov et al., 1996 and 1998; Dachev et al., 1998) at low L values after the SPE on 22 March 1991. This feature was observed by us till the middle of 1993.*

The next 4 space experiments were performed with Liulin type Deposited Energy Spectrometers (DES), which measured the spectrum (in 256 channels) of the deposited energy in a silicon detector from primary and secondary particles inside and outside of the ISS. The DES is a Liulin type (Dachev et al. 2002) miniature spectrometer-dosimeter containing one semiconductor detector, one charge-sensitive preamplifier, 2 or more microcontrollers and a flash memory. Pulse analysis technique is used for the obtaining of the deposited energy spectrum, which further is used for the calculation of the absorbed in the silicon detector dose and flux. The unit is managed by the microcontrollers through a specially developed firmware. Plug-in links provide the transmission of the stored in the flash memory data toward a standard Personal Computer (PC) or toward the telemetry system of the carrier. DES sensitivity was proved against neutrons and gamma radiation (Spurny and Dachev, 2002, 2009), which allows monitoring of the natural background radiation also.

For the analysis of REP the following DES on ISS were used:

- The Liulin-E094 instrument, which was a part of the experiment Dosimetric Mapping-E094, headed by Dr. G. Reitz that was placed in the US Laboratory Module of the ISS as a part of the Human Research Facility of Expedition Two, Mission 5A.1 in May-August 2001 (Reitz et al., 2005; Dachev et al., 2002, 2006; Nealy et al., 2007; Wilson et al., 2007; Slaba et al., 2011). The Liulin-E094 instrument contains 4 battery operated Mobile Dosimetry Units (MDU), which were placed inside the Destiny and Node-1 modules behind different shieldings above 10 g cm^{-2} ;
- The Liulin-MKS instrument (Dachev et al., 2005), which was launched to ISS in September 2005, is very similar to the Liulin-E094 instrument. The 4 MDUs were situated in different palaces of the Russian segment of ISS in 2008. It is still operable;
- The Radiation Risks Radiometer-Dosimeter (R3D) (Häder and Dachev, 2003), modification ‘E’ - R3DE, which was a part of the EXPOSE-E facility on the European Technological Exposure platform (EuTEF) (Figure 1.). It worked outside of the European Columbus

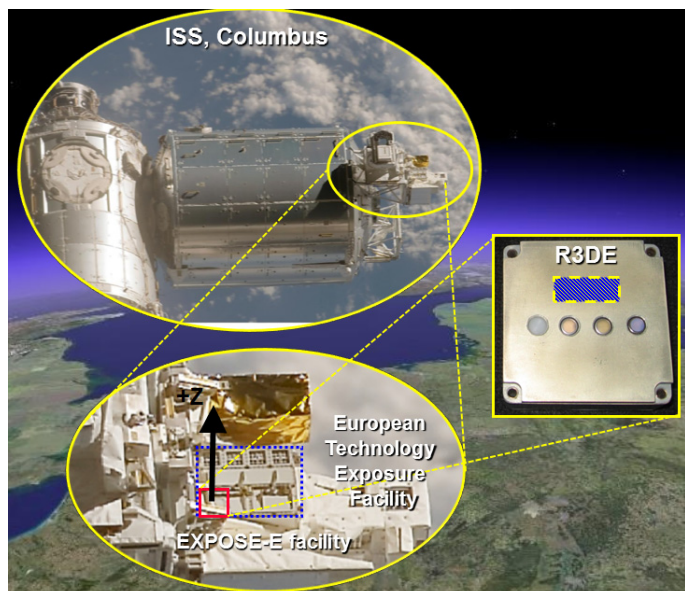


Fig. 1. The R3DE instrument worked successfully as part of the EXPOSE-E facility on the EuTEF platform outside the ISS Columbus module between February 2008 and September 2009.

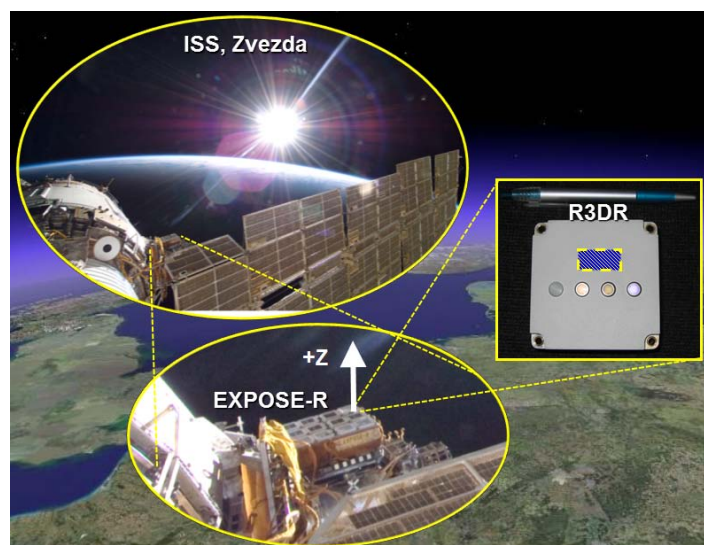


Fig. 2. The R3DR instrument worked successfully on the outside platform of the Russian Zvezda module of the ISS as a part of the EXPOSE-R facility between March 2009 and August 2010.

module of the ISS between 20th of February 2008 and 1st of September 2009 with a 10 seconds resolution behind less than 0.4 g.cm⁻² shielding;

- The R3DR spectrometer was launched inside of the EXPOSE-R facility on the ISS in December 2008 and was mounted at the outside platform of the Russian Zvezda module of the ISS (Figure 2.). The first data were received on March 11, 2009. Until the end of August 2010 the instrument worked almost permanently with a 10 seconds resolution and the data were recorded on the ISS.

The construction of the R3DE/R front panel consists of a 1.0 mm thick aluminum shielding in front of the detector. The total shielding of the detector is formed by an additional internal constructive shielding of 0.1 mm copper and 0.2 mm plastic material. The total external and internal shielding in front of the detector of the R3DE/R devices was 0.41 g cm⁻². The calculated stopping energy of normally incident particles to the detector is 0.78 MeV for electrons and 15.8 MeV for protons (Berger et al., 2012). This means that only protons and electrons with energies higher than the above mentioned could reach the detector.

The amplitudes of the fluxes and doses with the Liulin-E094 MDUs are smaller than the R3DE/R amplitudes because the additional shielding by the walls of the ISS, but all radiation sources are well seen in both locations.

3. Scientific results

3.1 Data selection procedure

The data selection procedure was developed so that to distinguish between the three expected radiation sources: (i) GCR particles, (ii) protons with more than 15.8 MeV energy in the SAA region of the inner radiation belt, and (iii) relativistic electrons with energies above 0.78 MeV in the ORB. Heffner (1971), Dachev (2009) and Dachev et al., (2012a, 2012b) showed that the dose to flux ratio (D/F) can characterize the type of the predominant radiation source in the Liulin type instruments in the near Earth radiation field. It was shown that the SAA and ORB data, which have relatively high fluxes, can be split in two parts by the simple relation of the dose to flux ratio based on the fact that one inner radiation belt proton with energy in the range 15.8–200 MeV can deposit in the detector between 6.5 and 1.08 nGy cm² particle⁻¹, whereas one outer radiation belt relativistic electron with energy in the range 1–10 MeV can deposit between 0.3 and 0.35 nGy cm² particle⁻¹ because of the much smaller mass. GCR protons in the equatorial and the low latitude regions have very small fluxes of less than 1 particle cm⁻² s⁻¹ that is why the D/F ratio is in these regions not stable and vary in the range from 0.03 and 30 nGy cm² particle⁻¹ (please look Figure 5 of Dachev et al., 2012b) so the D/F ratio is not applicable for the characterization of the GCR radiation source. For bremsstrahlung X-rays the dose-to-flux ratio is less than the electron ratio.

3.2 Dynamics of the “Mir” Space Station internal radiation environment for 19-30 June 1991 as measured by the LIULIN instrument

Figure 3 presents in 3 panels the dynamics of the “Mir” Space Station internal radiation environment for 19-30 June 1991 as measured by LIULIN instrument during high solar activity and high geomagnetic activity. All 3 panels are plotted against L value (McIlwain, 1961; Heynderickx et al., 1996) on the X axes. L corresponds to the equatorial radius of a magnetic drift shell in the case of a dipole field. The orbital parameters of the “Mir” space station and the ISS used in this paper are calculated by the KADR-2 software (Galperin et al., 1980.). Organizing the data in this way one can show the different particle populations and how they are distributed in the near-Earth space. The upper panel (Fig.3a) contains data for the measured dose rate values higher than 15 μGy h⁻¹. The middle panel (Fig.3b) is devoted to the Flux data, while the bottom panel (Fig.3c) presents the D/F ratio.

Four different radiation sources are visually distinguished in the data presented in Fig. 3b and 3c: Galactic cosmic rays (GCR), SAA (inner belt) protons, outer radiation belt (ORB) electrons and the new radiation belt (New). The GCR source is

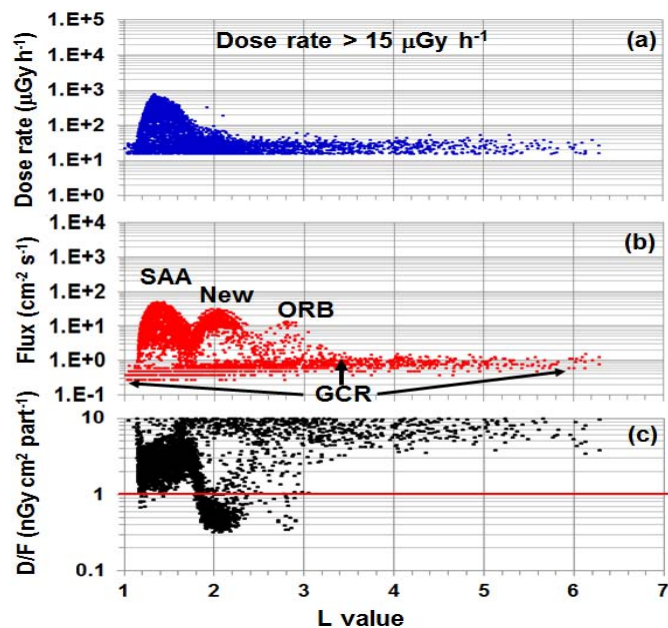


Fig. 3. Dynamics of the “Mir” SS internal radiation environment for 19-30 June 1991 as measured by LIULIN instrument.

seen in the bottom area of the Fig. 3a with dose rates between 15 and 40 $\mu\text{Gy h}^{-1}$. The GCR source produces the bunch of points around 6 $\text{nGy cm}^2 \text{particle}^{-1}$ seen in Fig 3b.

The maximum at the left side of Fig. 3a and 3c is generated mainly by inner radiation belt protons in the region of the SAA for L values less than 1.6. This maximum reached the highest dose rate and flux values seen in Figures 3a and 3b. The behavior of the D/F ratio in Figure 3c gives information about the particle population in the maximum. Almost all of the D/F values are greater than 1 $\text{nGy cm}^2 \text{particle}^{-1}$ (this value is emphasized on the figure by a heavy red line.), which according to the Heffner's (1971) findings corresponds to energetic protons. The D/F values to the left of the maximum, being in the North-West side of the SAA, are the smallest, while the right side values are the highest. This means that the effective proton energy decreases from about 100 MeV down to 20 MeV.

Another source starts to contribute to the doses and fluxes in the range of L values from 1.7 to 2.4, peaking at L=2.1. This source is recognized in Fig. 3b as a well seen maximum with a larger density of points with values 20-30 $\text{cm}^2 \text{s}^{-1}$. In Fig 3c this source is seen as a minimum with values between 0.3 and 0.8 $\text{nGy cm}^2 \text{particle}^{-1}$. These values of the D/F ratio correspond to an electron and/or a bremsstrahlung radiation source. Our previous investigations (Petrov et al., 1993 and 1994; Shurshakov et al., 1996; Dachev et al. 1998) associated it with the "New" radiation belt, first reported by Mullen et al. (1991). The particles in the "New" radiation belt were injected into the magnetosphere during the sudden commencement of magnetic storms (SSC) at 03:42 UT, 24 March 1991, and were further stably trapped for a long time. The "New" radiation belt was observed by us till the middle of 1993 (Dachev et al., 1998). The formation of the "New" radiation belt and the magnetosphere phenomena in 1991 are well seen in the >2.5 MeV data of the RDM instrument on the Japanese satellite EXOS-D <http://www.stp.isas.jaxa.jp/akebono/RDM/rdm/old/rdmflux1991.gif> (AKEBONO RDM data were provided through DARTS at the Institute of Space and Astronautically Science (ISAS, Japan.).

The right-most maximum seen in Figure 3b at L values equal to 2.8 is the Other Radiation belt (ORB) maximum, which also is generated by relativistic electrons. It is quite possible that we see only part of their flux and the bremsstrahlung by them. This is manifested by the smaller than 1 $\text{nGy cm}^2 \text{particle}^{-1}$ values of the D/F ratio in Figure 3c. The ORB maximum is situated at relatively very low L values because: 1) This was the tendency in June 1991 (Please look <http://www.stp.isas.jaxa.jp/akebono/RDM/rdm/old/rdmflux1991.gif>); 2) The measurements were performed inside "Mir" SS behind a large shielding and this allows the penetration only of very high energy electrons, trapped at relatively small L values (Dachev et al., 2009).

3.2 Dynamics of the ISS internal radiation environment for 12-30 May 2001 as measured by Liulin-E094 - MDU #2 instrument

Figure 4 presents in 3 panels the dynamics of the ISS internal radiation environment for 12-30 May 2001 as measured by Liulin-E094 - MDU #2 instrument. New here is that the measurements were performed by a Deposited Energy Spectrometer (DES) developed especially for the Dosimetric mapping experiment (Reitz et al., 2005). This DES measured the spectrum (in 256 channels) of the deposited energy in a silicon detector (Dachev et al., 2002).

The data were obtained with MDU#2, situated for the period 12th – 30th May 2001 in one of the less shielded places of the US laboratory module called "US Lab – Open rack overhead seat track in Retention Net". The battery operated cigarette box size MDU was very close to the US lab wall orientated with the detector toward the wall. Data presented by Dachev et al. (2006) are obtained with the same MDU but that paper deals mainly with the South Atlantic Anomaly (SAA) inner belt high energy proton distribution.

Despite the maximum of the solar activity cycle the observational period is characterized with relatively quiet geomagnetic conditions. The format of the figure is the same as that of Figure 3. The main findings from Figure 4 are as follow:

- In comparison with Fig. 3a and 3b the

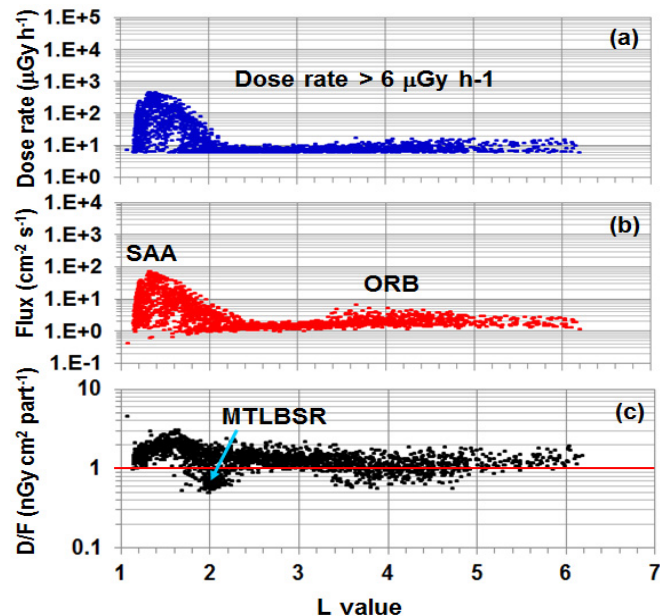


Fig. 4. Dynamics of the ISS internal radiation environment for 12-30 May 2001 as measured by Liulin-E094 MDU #2 instrument.

SAA maximum was extended in polar direction up to $L=2.2-2.5$. Our explanation is connected with the smaller shielding of MDU#2 in comparison with LIULIN shielding. This allowed the relatively low energy protons in the South-East edge of SAA to penetrate through the ISS walls and to reach the detector. The SAA D/F ratio seen in Figure 4c did have very similar values to those presented in Figure 3c, which is connected with the stably trapped proton population in the core of the SAA;

- On the place of the “New” belt at $1.8 < L < 2.2$ it is observed a “Middle term leaving belt in the slot region (MTLBSR)” (Zhang et al., 2006). When we plotted the locations of these events in geographic coordinates we found that they are situated as a belt in the south-east direction from the SAA maximum. Our explanation of these very low specific depositions is that we recorded the bremsstrahlung from the relativistic electrons outside the station. The electrons with energy of 10 MeV have only 22 mm stopping path in aluminum (Berger et al, 2012) and are not able to cross all shielding materials and to reach the detector of the MDU;
- In Fig. 4b we observe a bunch of points in the range of L values between 3.5 and 5 with flux values up to $5 \text{ cm}^{-2} \text{ s}^{-1}$. These points do not have adequate high values of dose rates in Fig. 4a. Our interpretation is that these higher flux points are the Bremsstrahlung signatures of ORB relativistic electrons, because their D/F ratio seen in Fig. 4c is between 0.6 and $0.8 \text{ nGy cm}^2 \text{ part}^{-1}$.

3.3 Dynamics of the ISS external radiation environment for 11-20 March 2008 and 1-10 April 2010 as measured by R3DE/R instruments

Figures 5 and 6 present data from the R3DE/R instruments, which were irradiated outside the ISS during the minimum of the solar cycle and quiet geomagnetic activity in 2008 and quiet but with an isolated major storm in 2010. The detailed position of the instruments is seen in Fig. 1 and 2. All 6 panels of the figures are plotted in the same way as the already described Figure 3. Main findings from Figure 5 and 6 are as follow:

- Both figures represent very similar distributions in the dependence on the L value, which in comparison with Figures 3 and 4 don't have any long of middle term leaving belts in the slot region. Only SAA and ORB regions are observed;
- The SAA flux and dose rates in both cases are higher than those in Figures 3 and 4, and the SAA maximum in April 2010 in Figure 6 is the highest observed. The reason of R3DR SAA fluxes and dose rates to be higher than those of R3DE can be inferred from Figure 1 and 2, which present the distribution of the masses in the surrounding environment of the R3DE and R3DR instruments on the ISS. R3DE was located inside the EXPOSE-E facility at the top of the EuTEF platform outside the European Columbus module. In Figure 1 the lower end of the heavy arrows pointing “up” (along the Earth radius in +Z direction) shows the exact place of the instrument. It is seen that R3DE was surrounded by the EXPOSE-E facility, and by different constructional elements of the EuTEF platform, and the Columbus module. All these

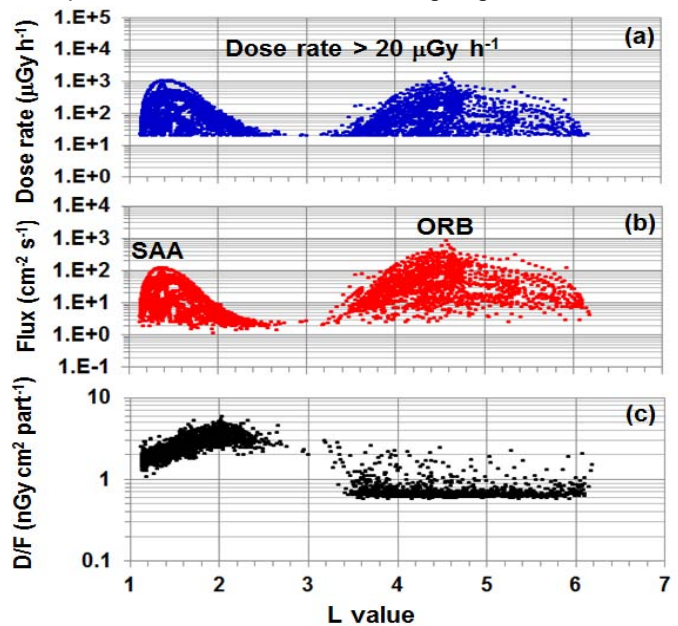


Fig. 5. Dynamics of the ISS external radiation environment for 11-20 March 2008 as measured by R3DE instrument.

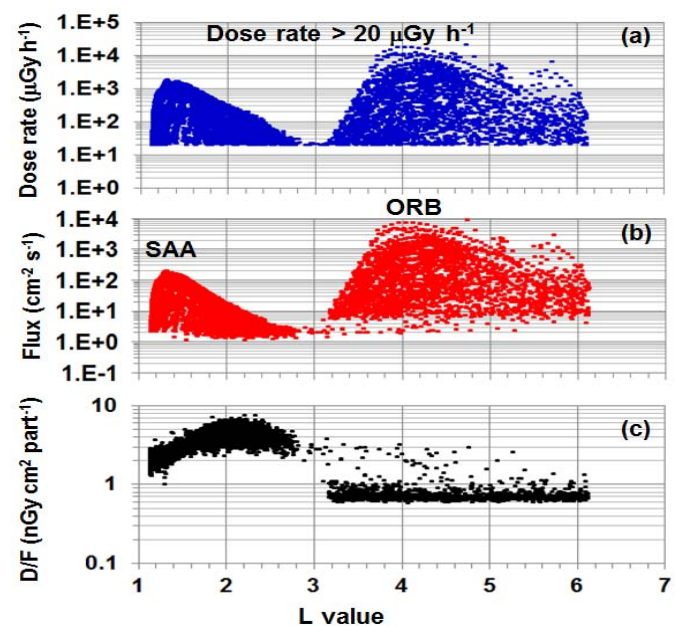


Fig. 6. Dynamics of the ISS external radiation environment for 1-10 April 2010 as measured by R3DR instrument.

surrounding masses produced additional shielding of the instrument against the SAA proton flux in the energy range of 15.8-200 MeV. The R3DR position presented in Figure 2 shows that this instrument was far from the Zvezda module body seen in the left part of the upper photograph, at the far end of the EXPOSE-R facility. It was shielded practically only by the EXPOSE-R facility from below, because the solar panels seen in the bottom of Figure 3b don't have large mass;

- The ORB flux and dose rate maxima in both figures are well situated at L values between 3 and 6 and the values are much higher than those in Figures 3 and 4 because both instruments were shielded only by their own constructional elements of 0.41 g cm^{-2} . Again the R3DR flux and dose rate values in the ORB are the highest observed. Not only because the minimal shielding but also because the very strong REP, which occurred on 7th of April 2010 being the second largest in GOES history with a $>2 \text{ MeV}$ electron fluence event (see Figure 1 of Dachev et al., 2012c). The fact that in Figures 5c and 6c the majority of points of the D/F ratio do have values below $1.0 \text{ nGy cm}^2 \text{ particle}^{-1}$ confirms the hypothesis that these particles are relativistic electrons. The rare points with D/F ratio higher than $1.0 \text{ nGy cm}^2 \text{ particle}^{-1}$ belong to GCR particles, for which the requirements dose rate to be larger than $20 \mu\text{Gy h}^{-1}$ is not enough strong to be excluded from the selection;
- The position of the R3DE ORB maximum in Figure 5 is at L equal to 4.5, while the R3DR ORB maximum is almost at $L=4$. This is because the R3DR data are taken between 1 and 10 of April 2010 i.e. relatively soon after the REP event on 7th of April, when the ORB is still situated at smaller L values. Further with the development in time of the REP event the ORB maximum tendency is to move at highest L values as seen in Figure 5. This process of movement is well seen in the $>2.5 \text{ MeV}$ data of RDM instrument on the Japanese satellite EXOS-D. <http://www.stp.isas.jaxa.jp/akebono/RDM/rdm/rdmflux2010.gif> and in Figure 9 of Dachev et al., (2012b). (AKEBONO RDM data were provided through DARTS at Institute of Space and Astronautically Science (ISAS), Japan.)

3.4 Variations of the SAA ISS radiation environment

Figure 7 presents extended view of the SAA D/F profiles seen in Figures 4c-6c in the L values range between 1.1 and 1.6. Data are separated in 3 panels. Data in Figures 7b and 7c are with 10 s resolutions while Figure 7a is with a 30 s resolution, that is why the number of points seen there is much smaller. The heavy line in the 3 panels presents the calculated linear fits over the data. The minimal and maximal values of the linear fits are used for calculations by Heffner's formulae (Heffner 1971) of the average SAA proton energies.

Figure 7a presents the D/F data taken by the Liulin-E094 MDU#2 with a 30 seconds resolution and seen also in Figure 4c. Despite that MDU#2 was situated in one of the less shielded places of the US laboratory module we recognize them as the most shielded data because the D/F values are the smallest and respectively the calculated by Heffner's formulae (Heffner 1971) proton energies are the highest (please look at Table 1.).

Figures 7b and 7c present the R3DE/R data and together with the calculated values of the average proton energies (Table 1) confirm again that the R3DR instrument is less shielded than the R3DE instrument.

In Table 1 the last column shows the poleward flux boundary, which also characterizes the amount of shielding in front of the detector because with the increase of the L value the energy of the trapped in the SAA protons decreases as seen in Figure 7.

The exact dynamics of the movements of the dose rate boundary during descending and ascending orbits of ISS is presented in Figure 8. Full resolution dose rate data from Liulin-MKS MDU#4, NASA TEPC (Badhwar et al., 1996) and R3DE

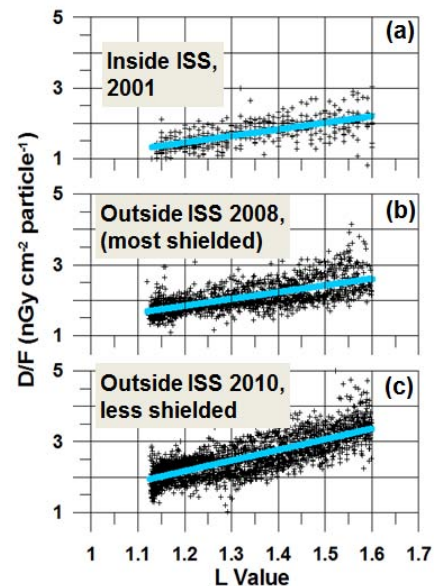


Fig. 7. Variations of the SAA ISS D/F ratios in dependence by the thickness of the shielding.

Table 1. Comparison of the D/F values and calculated by Heffner's formulae proton energies (Heffner 1971) for the 3 instruments on ISS.

Instrument/ parameter	D/F min [nGy cm ⁻² particle ⁻¹]	E min [MeV]	D/F max [nGy cm ⁻² particle ⁻¹]	E max [MeV]	Dose boundary of ISS [L]
MDU#2	1.4	86	2.3	38	2.2
R3DE	1.65	64	2.6	32	2.6
R3DR	1.95	49	3.45	22	2.8

instruments as measured on 14th of July 2008 are plotted in dependence on the UT. The lower panel contains data from Liulin-MKS MDU#4 and R3DE instruments while the upper is devoted to the NASA TEPC instrument data obtained from NASA GSFC, by 'Coordinated Data Analysis Web' at Goddard Space Flight Center, <http://cdaweb.gsfc.nasa.gov/tmp/> (Zapp, 2013). Both panels are plotted in identical dose rate Y axes over the X axes, which is UT on 14th of July 2008 between 00:00 and 09:00.

The meander in the range 0.1-15 $\mu\text{Gy h}^{-1}$ was generated by registration of the dose rates from GCR, while the maximums reaching 1553 $\mu\text{Gy h}^{-1}$ were obtained in the region of the SAA. The comparison of all 3 curves shows that they are very similar and the reason is that they follow the variations of the L value seen in the bottom panel. The following peculiarities have to be mentioned: 1) The SAA dose rates outside ISS were greater than inside because of the shielding of the stations walls. For example the R3DE (outside ISS) maximal dose rate in the first SAA maximum was 1553 $\mu\text{Gy h}^{-1}$, while the NASA TEPC and Liulin-MKS MDU#4 instruments reached 973 and 701 $\mu\text{Gy h}^{-1}$ respectively; 2) The GCR dose rates inside the station are greater than outside because of the additional doses generated by secondary particles in the walls of the station (Damasso et al., 2009; Dachev, 2013). The highest SAA dose rates were observed (as expected) in the R3DE instrument data. The lowest were seen in the Liulin-MKS MDU#4 data, which seems to be in a heavier shielded location than the NASA TEPC instrument. The GCR averaged doses, which were selected from the 3 instruments from the data below 10 $\mu\text{Gy h}^{-1}$ are ordered as follows: R3DE 2.68 $\mu\text{Gy h}^{-1}$, Liulin-MKS MDU#4 3.93 $\mu\text{Gy h}^{-1}$, and NASA TEPC 4.3 $\mu\text{Gy h}^{-1}$. The higher GCR dose rates in Liulin-MKS MDU#4 instrument are well seen in the lower panel of Figure 8.

The movements of the poleward dose rate boundary can be seen very well in the lower panel by comparison of the curves inside the SAA maximums. The first 2 (from the left) SAA maximums were measured over descending orbits (increasing L values in the SAA region seen on the lower panel), which cross the equator at approximately -70° , -94° and -108° West longitude. In these cases the poleward boundary was at the left side of the SAA maximum. This is seen as a more extended R3DE left side of the SAA maximum, because, being in less shielding, protons with lower energies can reach the detector. The decreasing energies of the protons calculated on the base of Heffner's equations (Heffner, 1971) are also well seen on the lower panel of Figure 8.

The last 2 (from the left) SAA maximums were measured over ascending orbits (decreasing L values in the SAA region). In these cases the poleward boundary was at the right side of the SAA maximum. This is seen as a more extended R3DE right side of the SAA maximum. The increasing energies of the protons are not so steep because of the relatively small gradient of the L value decrease.

The last 2 (from the left) SAA maximums were measured over ascending orbits (decreasing L values in the SAA region). In these cases the poleward boundary was at the right side of the SAA maximum. This is seen as a more extended R3DE right side of the SAA maximum. The increasing energies of the protons are not so steep because of the relatively small gradient of the L value decrease.

4. Conclusions

This paper analyzed the data obtained in the different radiation environments of galactic cosmic rays, inner radiation belt trapped protons in the region of the South Atlantic Anomaly and outer radiation belt relativistic electrons during measurements with the Bulgarian built instruments on "Mir" SS and ISS. Special attention was paid to the REP variations.

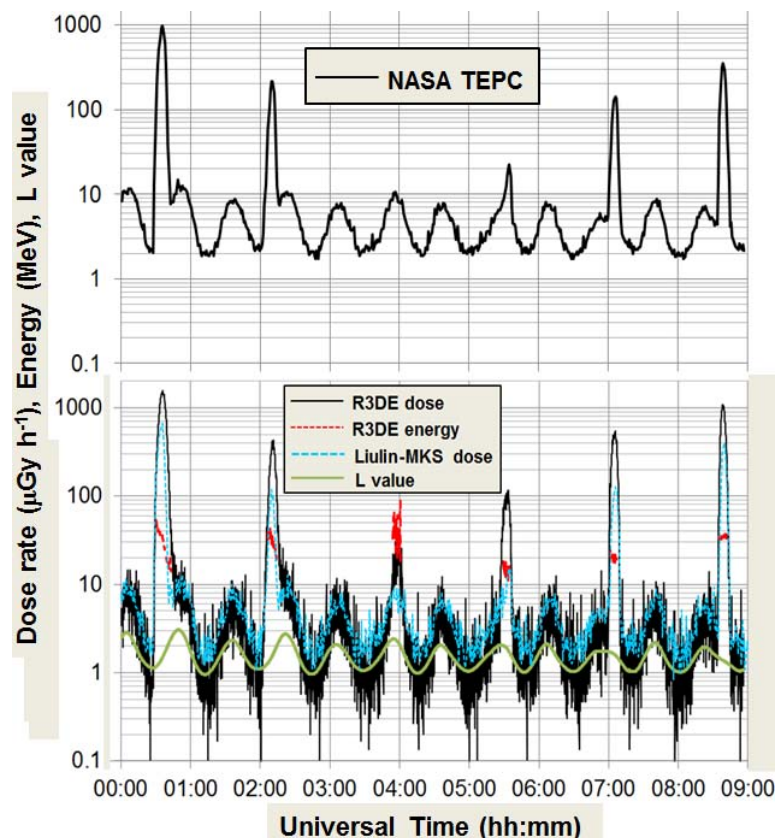


Fig. 8 Comparison of the dose rates obtained on 14th of July 2008 by Liulin-MKS MDU#4 (Inside ISS at bottom panel), NASA TEPC (Inside ISS at top panel) and R3DE (outside ISS at bottom panel) instruments. The obtained with R3DE proton energies in the SAA and the L value are also shown in the bottom panel.

The Liulin-MKS, Liulin-E094 and R3DE/R, low mass, dimension and price instruments, proved their ability to characterize the inside and outside manned spacecraft radiation environment including the relativistic electron precipitations. This was achieved mainly by the analysis of the dose to flux ratios and deposited energy spectra, which were obtained in each measurement cycle of 30 or 10 seconds.

The main conclusion is that the REP events are common on the "Mir" SS and ISS. In the case of measurements inside the station the REP observations were mainly indirect because of the walls shielding, which stopped the major amount of the less energetic relativistic electrons. Never the less the formation of different long and middle term radiation belts was monitored and analyzed. In the case of measurements outside the station the measured instant relativistic electrons dose rates can reach values even larger than $20,000 \mu\text{Gy h}^{-1}$. Although the obtained long term doses do not pose extreme risks for astronauts being on EVA they have to be considered as a permanently observed source, which requires additional comprehensive investigations.

The obtained higher doses produced by the SAA protons and ORB electrons sources in the R3DR instrument is the main finding of the presented data. We explain this with fact that this instrument was less shielded by surrounding construction elements of the Russian Zvezda module than the R3DE instrument being surrounded by heavy construction elements of the EuTEF platform and European Columbus module.

The GCR dose rate measured with the R3DE instrument is larger for the whole period between March and June 2009 than the observed by the R3DR instrument contrary to the dose rates obtained for the SAA and ORB. By comparison with the Foton-M3 data we prove that this higher dose rates were produced by the additional dose rate generated by secondary particles in the heavily shielded R3DE instrument. In the future this fact can be further proved using of calculations based on theoretical models.

The main conclusion from the study is that the values of the dose rates produced by different radiation sources around the ISS do have large and fast dynamics in space and time. All data obtained outside the station can be interpreted as possible doses obtained by the cosmonauts and astronauts during EVA because the R3DE/R instruments shielding is very similar to the Russian and American space suits average shielding (Anderson et al. 2003; Benton et al., 2006; Shurshakov et al., 2009). Fast, active measurements at the body of each astronaut to obtain the exact dynamics of the dose accumulation during EVA are required.

An instrumental solution was foreseen by Dachev et al. (2011b) where the possible hardware and software improvements for a new Liulin type dosimeter were proposed. On the base of the analysis of the deposited energy spectrum's shape and the value of the dose to flux ratio the new instrument will be able to distinguish the different kind of radiation sources in the ISS radiation environment as GCR, inner radiation belt protons and outer radiation belt electrons. It will measure, calculate, store and present on a display the fast variations of the absorbed and ambient dose equivalent (Ploc et al., 2010) in any of the possible surrounding mass distribution. This will finally give the necessary active measurements of the radiation dose rates during EVAs, which were proposed more than 10 years ago by NCRP, Report No. 142 in 2002.

5. Acknowledgements

This work is partially supported by the Bulgarian Academy of Sciences and contract DID 02/8 with the Bulgarian Science Fund.

References:

1. B a d h w a r , G. D., et al., In-flight radiation measurements on STS-60, Rad. Meas., 17–34, [http://dx.doi.org/10.1016/1350-4487\(95\)00291-X](http://dx.doi.org/10.1016/1350-4487(95)00291-X), 1996.
2. B a d h w a r , G. D., et al. Radiation environment on the "Mir" orbital station during solar minimum. Adv. Space. Res. 22 (4), 501-510, 1998.
3. B e n t o n , E. R. and B e n t o n , E. V. Space radiation dosimetry in low-Earth orbit and beyond, Nucl. Instrum. and Methods in Physics Research, B, 184, (1-2), 255-294, 2001.
4. B e r g e r , M. J. , C o u r s e y , J. S. , Z u c k e r , M. A. , and C h a n g , J. Stopping-Power and Range Tables for Electrons, Protons, and Helium Ions. NIST Standard Reference Database 124. Available online at: <http://physics.nist.gov/PhysRefData/Star/Text/contents.html>, May 2012.
5. D a c h e v , T s. P. , Y u. N. M a t v i i c h u k , J. V. S e m k o v a , R. T. K o l e v a , B. B o i c h e v , P. B a y n o v , N. A. K a n c h e v , P. L a k o v , Y a. J. I v a n o v , P. T. T o m o v , V. M. P e t r o v , V. I. R e d k o , V. I. K o j a r i n o v , R. T y k v a , Space radiation dosimetry with

- active detections for the scientific program of the second bulgarian cosmonaut on board the "Mir" space station, *Adv. Space Res.*, 10, 247-251, [http://dx.doi.org/10.1016/0273-1177\(89\)90445-6](http://dx.doi.org/10.1016/0273-1177(89)90445-6), 1989.
6. Dachev, Ts.P., J.V.Semkova, Yu.N.Matviichuk, B.T.Tomov, R.T.Koleva, P.T.Baynov, V.M.Petrov, V.V.Shurshakov, Yu.Ivanov, Inner Magnetosphere Variations after Solar Proton Events. Observations on "Mir" Space Station In 1989-1994 Time Period, *Adv. Space Res.*, 22, 521-526, [http://dx.doi.org/10.1016/S0273-1177\(98\)01073-4](http://dx.doi.org/10.1016/S0273-1177(98)01073-4), 1998.
 7. Dachev, Ts., Tomov, B., Matviichuk, Yu., Dimitrov Pl., Lemaire, J., Gregoire, Gh., Cyamukungu, M., Schmitz, H., Fujitaka, K., Uchihori, Y., Kitamura, H., Reitz, G., Beaujean, R., Petrov, V., Shurshakov V., Benghin, V., Spurny, F. Calibration results obtained with Liulin-4 type dosimeters, *Adv. Space Res.* 30, 917-925, doi:10.1016/S0273-1177(02)00411-8, 2002.
 8. Dachev, T., Atwell, W. Semones, E.; Tomov, B., Reddell, B. ISS Observations of SAA radiation distribution by Liulin-E094 instrument on ISS, *Adv. Space Res.*, 37, 1672-1677, doi:10.1016/j.asr.2006.01.001, 2006.
 9. Dachev, Ts., Pl. Dimitrov, B. Tomov, Yu. Matviichuk, New Bulgarian Build Spectrometry-Dosimetry Instruments – Short Description, Proceedings of 11-th International Science Conference on Solar-Terrestrial Influences, pp 195-198, Sofia, November 23-25, <http://www.stil.bas.bg/11conf/Proc/195-198.pdf>, 2005.
 10. Dachev, Ts.P., Tomov B.T., Matviichuk Yu.N., Dimitrov P.G., Bankov N.G. Relativistic Electrons High Doses at International Space Station and Foton M2/M3 Satellites, *Adv. Space Res.*, 1433-1440, doi:10.1016/j.asr.2009.09.023, 2009.
 11. Dachev, Ts.P., Characterization of near Earth radiation environment by Liulin type instruments, *Adv. Space Res.*, 1441-1449, doi:10.1016/j.asr.2009.08.007, 2009.
 12. Dachev, Ts., Horneck G., Häder D.-P., Lebert M., Richter P., Schuster M., Demets R. Time profile of cosmic radiation exposure during the EXPOSE-E mission: the R3D instrument. *Journal of Astrobiology*, 12, 5, 403-411, <http://eea.spaceflight.esa.int/attachments/spacestations/ID501800a9c26c2.pdf>, 2012a.
 13. Dachev, Ts.P., Tomov B.T., Matviichuk Yu.N., Dimitrov Pl.G., Bankov N.G., Reitz G., Horneck G., Häder D.-P., Lebert M., Schuster M. Relativistic Electron Fluxes and Dose Rate Variations during April-May 2010 Geomagnetic Disturbances in the R3DR Data on ISS. *Adv. Space Res.* 50, 282-292, <http://dx.doi.org/10.1016/j.asr.2012.03.028>, 2012b.
 14. Dachev, Ts., Tomov B.T., Matviichuk Yu.N., Dimitrov Pl.G., Bankov N.G., Reitz G., Horneck G., Häder D.-P., Lebert M., Richter P., Schuster M. Relativistic Electron Fluxes and Dose Rate Variations Observed on the International Space Station, (available online since 4 August 2012) in JASTP, <http://dx.doi.org/10.1016/j.jastp.2012.07.007>, 2012c.
 15. Dachev, Ts. Analysis of the space radiation doses obtained simultaneously at 2 different locations outside ISS. *Adv. Space Res.* paper ASR-D-13-00085, 2013. (under evaluation)
 16. Damasso, M., Dachev Ts., Falzetta G., Giardi M.T., Rea G., Zanini A. The radiation environment observed by Liulin-Photo and R3D-B3 spectrum-dosimeters inside and outside Foton-M3 spacecraft, *Radiation Measurements*, V. 44, N0 3, 263-272, doi:10.1016/j.radmeas.2009.03.007, 2009.
 17. Galperin, Yu.I., Ponomarev, Yu.N., Sinizin, V.M. Some Algorithms for Calculation of Geophysical Information Along the Orbit of Near Earth Satellites. Report No 544. *Space Res. Inst., Moscow*, 1980. (in Russian)
 18. Heffner, J., Nuclear radiation and safety in space, M, Atomizdat, pp 115, 1971. (in Russian).
 19. Heynderickx, D., Lemaire, J. and Daly, E. J. Historical Review of the Different Procedures Used to Compute the L-Parameter. *Radiation Measurements*. 26, 325-331, 1996.
 20. McIlwain, C. E. Coordinates for mapping the distribution of magnetically trapped particles. *J. Geophys. Res.*, 66, 3681-3691, 1961.
 21. Mewaldt, R.A. Cosmic Rays, available online at http://www.srl.caltech.edu/personnel/dick/cos_encyc.html, 1996.
 22. Mullen, E. G., Gussenhoven M.S., Ray K. and Violet M. A double-peaked inner radiation belt: cause and effect as seen on CRRES. *IEEE Trans. Nucl. Sci.* 38, 1713-1718, 1991.
 23. NCRP. Radiation Protection Guidance for Activities in Low Earth Orbit. Report No. 142, Bethesda, MD, 2002.
 24. Nealy, J.E., Cucinotta F.A., Wilson J.W., Badavi F.F., Zapp N., Dachev T., Tomov B. T., Semones E., Walker S.A., Angelis G. De, Blattnig S. R., Atwell W. Pre-engineering spaceflight validation of environmental models and the 2005 HZETRN simulation code. *Adv. Space Res.*, 40, 11, 1593-1610, doi:10.1016/j.asr.2006.12.030, 2007.

25. Petrov, V.M., Makhmutov V.S., Shurshakov V.A., Panova N.A. and Dachev Ts. Space distribution of particle fluxes and absorbed dose rate in SAA region according to "Mir" spaces station measurements *Isv. RAN, Phys. Ser.* 57, 100-103, 1993. (in Russian)
26. Petrov, M.V., V.S. Makhmutov, N.A. Panova, V.A. Shurshakov, Ts.P. Dachev, Ju.N. Matviichuk, J.V. Semkova, Peculiarities of the Solar Proton Events of October 19, 1989 and March 23, 1991 According to the Measurements On Board the "MIR" Space Station, *Adv. Space Res.*, 14, 645-650, [http://dx.doi.org/10.1016/0273-1177\(94\)90520-7](http://dx.doi.org/10.1016/0273-1177(94)90520-7), 1994.
27. Reitz, G., R. Beaujean, E. Benton, S. Burmeister, T. Dachev, S. Deme, M. Luszik-Bhadra, P. Olko, Space radiation measurements on-board ISS-The DOSMAP experiment, *Radiat. Prot. Dosim.* 116 (1-4), 374-379, 2005.
28. Shurshakov, V.A., S.L. Huston, Ts.P. Dachev, V.M. Petrov, Yu.V. Ivanov, J.V. Semkova, Direct comparison of transient radiation belt topology and dynamics in 1991 based on measurements onboard "Mir" Space Station and NOAA Satellite, *Adv. Space Res.*, vol. 22, No 4, pp. 527-531, 1998. [http://dx.doi.org/10.1016/S0273-1177\(98\)01074-6](http://dx.doi.org/10.1016/S0273-1177(98)01074-6)
29. Shurshakov, V.A., V.M. Petrov, Makhmutov, and Ts.P. Dachev, New radiation belt dynamics according to measurements made by "LIULIN" dosimeter-radiometer on board the "MIR" space station in 1991, *Radiation Measurements.* 26, No 3, 379-387, [http://dx.doi.org/10.1016/1350-4487\(96\)00040-6](http://dx.doi.org/10.1016/1350-4487(96)00040-6), 1996.
30. Simpson, J.A., in: Shapiro M.M. (Ed.) (1983) *Composition and origin of cosmic rays*, NATO ASI Series C: Mathematical and Physical Sciences. Vol. 107, Reidel, Dordrecht.
31. Slaba, T.C., Blattnig S.R., Badavi F.F., Stoffle N.N., Rutledge R.D., Lee, K.T., Zapp E.N., Dachev T.P. and Tomov B.T. Statistical Validation of HZETRN as a Function of Vertical Cutoff Rigidity using ISS Measurements. *Adv. Space Res.*, 47, 600-610, doi:10.1016/j.asr.2010.10.021, 2011.
32. Spurny, F., T. Dachev, On Board Aircrew Dosimetry with a Semiconductor Spectrometer, *Radiat. Prot. Dosim.* 100, pp 525-528, 2002.
33. Spurny, F., and T.P. Dachev, New results on radiation effects on human health, *Acta geophysica*, vol. 57, no. 1, pp. 125-140, 2009. DOI: 10.2478/s11600-008-0070-6
34. Wilson, J.W., Nealy J.E., Dachev T., Tomov B.T., Cucinotta F.A., Badavi F.F., Angelis G. De, Leutke N., Atwell W. Time serial analysis of the induced LEO environment within the ISS 6A. *Adv. Space Res.*, 40, 11, 1562-1570, doi:10.1016/j.asr.2006.12.030, 2007.
35. Zapp, NASA GSFC, by 'Coordinated Data Analysis Web' at Goddard Space Flight Center, <http://cdaweb.gsfc.nasa.gov/tmp/>, February, 2013.
36. Zheng, Y., Lui, A.T.Y., Li, X. and Fok, M.-C., Characteristics of 2-6 MeV electrons in the slot region and inner radiation belt, *J. Geophys. Res.*, 111, A10204, doi:10.1029/2006JA011748, 2006.